Materials Research Express

RECEIVED
24 May 2018

REVISED
23 June 2018

ACCEPTED FOR PUBLICATION
29 June 2018

PUBLISHED
11 July 2018

PAPER

Phase transition and optical absorption evolution of WO_3 nanoparticles induced by pressure

Jiaji Ruan[1], **Kunyapat Thummavichai**[2], **Yang Lu**[1], **Yanqiu Zhu**[2,3] and **Hao Yan**[1,3]

[1] Center for High Pressure Science & Technology Advanced Research, Shanghai 201203, People's Republic of China
[2] College of Engineering, Mathematics and Physical Sciences, University of Exeter, Exeter EX4 4QF, United Kingdom
[3] Authors to whom any correspondence should be addressed.

E-mail: y.zhu@exeter.ac.uk and yanhao@hpstar.ac.cn

Keywords: WO_3 nanoparticles, high pressure, Raman spectra, UV-Vis absorption spectra

Abstract

Tungsten trioxide (WO_3) has been investigated extensively because of its photochromic and electrochromic properties, which allow its color to be changed easily under various conditions. This research reports the pressure-induced chromism of WO_3 nanoparticles under pressures from ambient pressure to 31.8 GPa, in an effort to establish the pressure-structure-coloration relationship of WO_3 nanoparticles. *In situ* Raman spectra were used to evaluate the phase structures; and *in situ* UV–vis absorption spectra were utilised to characterise the coloration performance of the WO_3 nanoparticles. The phase transition and coloration characteristics of the nanoparticles were investigated in comparison with microcrystalline WO_3, based on the Raman results, and a series of phase transition sequences, associated with irreversible color change, was observed under different pressures.

1. Introduction

Tungsten trioxide (WO_3) is a type of hexagonal or cubic symmetrically structured semiconductor that has attracted immense research attention, because of its promising photochromic, electrochromic, and photocatalytic properties, etc [1–8]. After the first photochromism was discovered by S K Deb in 1973 [9], the preparation, properties, and structure investigations of WO_3 have been extensively carried out. Recent photochromism studies of WO_3 have mainly been focused on photochromism of WO_3 films, with promising potentials in applications in smart window to regulate the room temperature [10]. The electrochromism of WO_3 has huge potentials in television screens and windows to achieve tunable reflection coatings [11, 12]. Effects of crystallite size on these performances of WO_3 have increasingly attracted more research attention [13], and the extraordinary properties of nanocrystalline WO_3 make them particularly attractive in the construction of nano-electronic and nano-optoelectronic devices [14–16].

Micro-structured WO_3 has a large variety of phases under different pressures [17, 18]. Two stable structures with a triclinic phase ($P\bar{1}$) and monoclinic phase ($P2_1/n$) were found at ambient condition, respectively [19]. Xu *et al* [20] showed that the triclinic phase transferred to a new monoclinic phase ($P2_1/c$) above 0.57 GPa, based on x-ray diffraction (XRD) study. However, their result disagreed with Salje's study in 1980, which reported that both of the phases transformed to a monoclinic phase (Pc) [21]. Later on, Souza-Filho *et al* reported that the WO_3 microcrystals containing a mixture of triclinic phase ($P\bar{1}$) and monoclinic phase ($P2_1/n$) gradually transferred to a monoclinic phase ($P2_1/c$) and the phase transition was completed above 1.4 GPa, according to their Raman spectra [22]. Further increase the pressures, microcrystalline WO_3 underwent two weak structure transitions at 3 and 10 GPa and one phase transition from monoclinic phase ($P2_1/c$) to monoclinic phase ($P2_1/a$) at 22 GPa, based on Raman spectra and XRD study conducted by M. Boulova *et al* [23, 24]. However, the investigation towards nanoscale WO_3 under high pressure has rarely been reported.

In this article, we firstly use *in situ* Raman spectroscopic technique to study the structural features of WO_3 nanoparticles, against microcrystalline particles, under high pressures, then use *in situ* UV–vis technique to

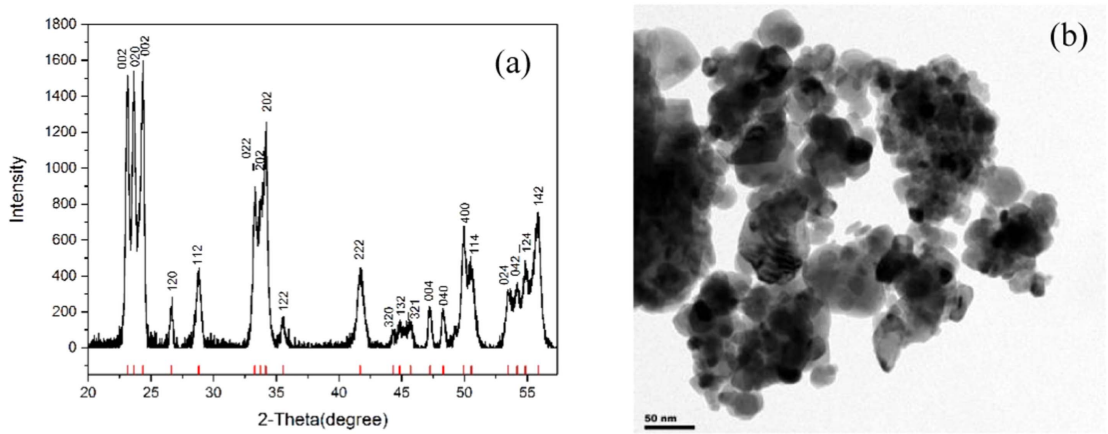

Figure 1. (a) X-ray diffraction spectra of WO_3 nanoparticles; (b) TEM picture of WO_3 nanoparticles.

assess the coloration behavior, and finally to establish the pressure-structure-coloration relationship of WO_3 nanoparticles.

2. Experimental

The WO_3 nanoparticles used in this study were obtained by using a simple heat treatment process. The precursor $W_{18}O_{49}$ bundled nanowires was prepared by using a solvothermal technique, as we have described previously [25]. After the $W_{18}O_{49}$ product was synthesized, 0.1 g of $W_{18}O_{49}$ was placed into a ceramic boat and annealed at 800 °C in air for 1 h, then continually annealed at 200 °C for another 1 h to achieve the WO_3 nanoparticles.

Since both the monoclinic phase ($P2_1/n$) and triclinic phase ($P\bar{1}$) are reportedly stable at room temperature [19], we characterized the sample by x-ray diffractometers produced by PANalytical with CuK_α radiation (40 kv and 40 mv). The particle size of the nanoparticles was assessed by using scanning electron microscopy (SEM) and transmission electron microscopy (TEM).

The WO_3 powder sample was compressed into a symmetric diamond anvil cell (DAC) with 300 μm-diameter anvil culet and T301 stainless steel gasket, and a 150 μm-diameter hole was drilled in the middle of the gasket as the sample chamber. The pressure-transmitting medium was silicon oil. A ruby granule was placed in the chamber to obtain the pressure with the ruby fluorescence line shift [26]. The pressure ranged from 0.3 to 31.9 GPa. Since below 290 K the monoclinic phase undergoes a phase transition to a triclinic phase [18, 19], all the experiments were therefore performed at room temperature.

The *in situ* Raman spectra were recorded with a Renishaw inVia spectrometer with a wavenumber range of 70 to 1000 cm^{-1}. The Nd:YAG laser was used to excite the sample. An Olympus 20× magnification microscope was used to focus the laser, and the diameter of the laser spot was about 2 μm. The incident power on the sample was 5 mW. The exposure time for each spectrum was 15 s. The accumulations were 2 times for 0–17 GPa, and 3 times above 17 GPa. The UV–vis absorption spectra were acquired on a micro HP UV–vis system (Ocean Optics). The tested wavelength ranged from 330 nm to 850 nm. The pressure ranged from 0.5 to 31.8 GPa.

3. Results

The XRD spectrum of the synthesized WO_3 nanoparticles at ambient pressure and room temperature is shown in figure 1(a), which matches well with ICDD-43-1035. Three main peaks of (002), (020) and (200) located at 2-theta degree of 23.10°, 23.63° and 24.34° respectively, which are used to identify the monoclinic phase ($P2_1/n$). No additional XRD peaks for the triclinic phase ($P\bar{1}$) were found. The average size of the particles was determined to be about 30 nm with TEM, as shown in figure 1(b).

Raman spectra of the two different pressure ranges are presented in figures 2(a) and (b), respectively. From 0 to 7.7 GPa (figure 2(a)), the spectrum of 0 GPa refers to sample prior to being loaded into the DAC. When the sample was loaded into the DAC and the pressure was increased to 0.3 GPa just for sealing, a phase transition had already been observed and new peaks E, F and G appeared. The same phenomenon has been reported in bulk WO_3 [21]. Further increase the pressure, peak D became weaker and was hardly observable; whereas, peak A was replaced by peak E, and two new peaks, H and I, replaced peaks B and C at 1.6 GPa, which indicates the complete of first phase transition around 1.6 GPa This phase transition point of WO_3 nanoparticles is the same to the

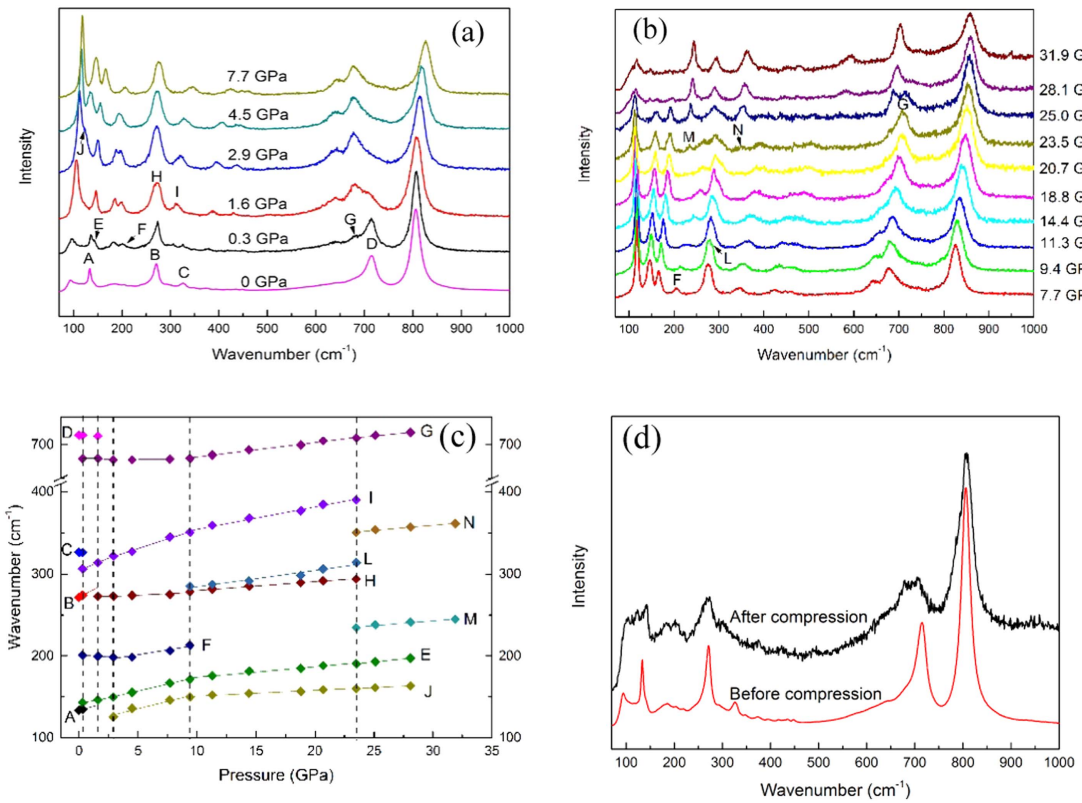

Figure 2. (a) Raman spectra under pressure from 0 to 7.7 GPa, (b) Raman spectra under pressure from 7.7 to 31.9 GPa, (c) wavenumbers of main Raman spectra peaks under different pressures and (d) Raman spectra before and after the compression.

Table 1. Phase of WO_3 nanoparticles [22–24].

Pressure (GPa)	Phase
Ambient	Monoclinic ($P2_1/n$)
0.3–1.6	Mixed phase of ($P2_1/n$) and ($P\bar{1}$)
1.6–2.9	Monoclinic ($P2_1/c$)
2.9–9.8	High pressure phase I
9.8–23.5	High pressure phase II
23.5-	Monoclinic ($P2_1/a$)

result of micro-sized WO_3 that was reported by Souza-Filho *et al* [22] The next phase transition took place at 2.9 GPa, as evidenced by the appearance of a new peak J. Two minor peaks around 200 cm^{-1} finally merged into one new peak at 4.5 GPa. Microcrystalline WO_3 has been reported a Raman spectral anomalies at about 3 GPa [23]. In the low-pressure region, phase transition before 1.6 GPa and at 2.9 GPa were recognized.

From 7.7 to 31.9 GPa (figure 2(b)), a new peak L was found, whilst peak F was hardly visible when the pressure was increased to 9.4 GPa. This indicates the phase transition which has previously been reported as a weak structure transition for the microcrystalline WO_3 [23]. Further pressure increases up to 23.5 GPa resulted in only peak shift whilst the spectra remained the same. At 23.5 GPa, new peaks M and N were visible, and at 28.1 GPa peak G became hardly observable. In the medium pressure region, 9.4 GPa and 23.5 GPa have been recognized as the phase transition points. Both transition points have previously observed in micro-sized WO_3, with peak G at 28.1 GPa [23]. From these Raman observations, it seems that the pressure-induced phase transition behavior of WO_3 nanoparticles is similar to those of micro-sized WO_3. The wavenumbers of peaks we marked under different pressure are showed in the figure 2(c). The phase of WO_3 nanoparticles under different pressure are presented in table 1. The mixed phase includes monoclinic phase ($P2_1/n$) and triclinic phase ($P\bar{1}$) [22]. At the same time, the high pressure phase I and II are still uncertain and need to be judged with further XRD study. Figure 2(d), before and after the compression, exhibits different Raman spectroscopic features of the WO_3 nanoparticles, which demonstrates the irreversible nature of the pressure-induced phase transition.

Figure 3 shows the UV–vis absorption spectra of the WO_3 nanoparticles under various pressures, which is also presented as two parts for an easy comparison with the Raman data (figure 2). At 0.5 GPa, the absorption

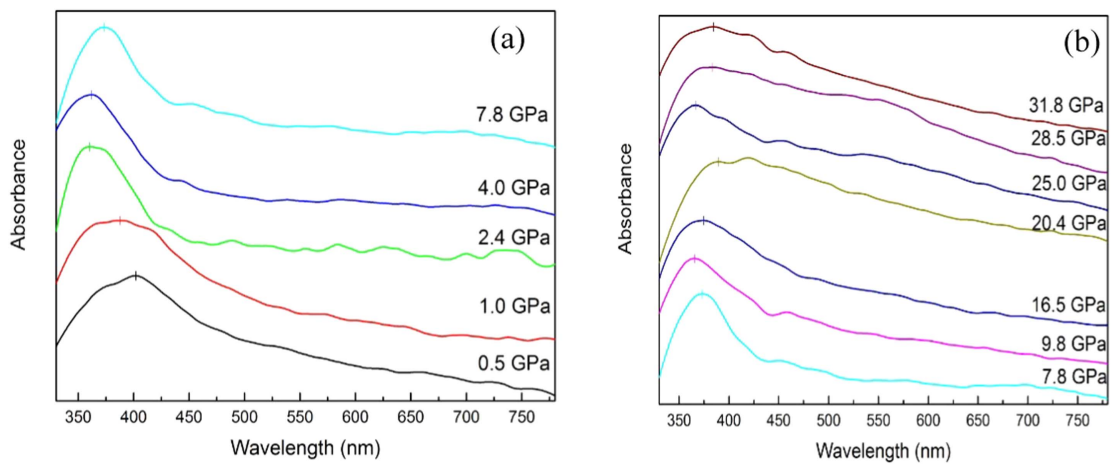

Figure 3. UV–vis absorption spectra of WO_3 nanoparticles obtained at different pressure ranges: (a) 0.5–7.8 GPa. (b) 7.8–31.8 GPa.

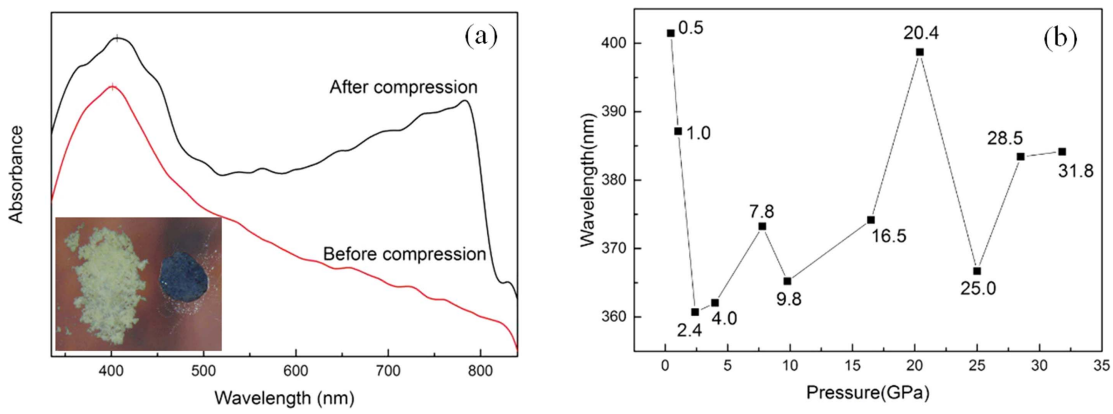

Figure 4. (a) UV–vis absorption spectra of WO_3 nanoparticles and their corresponding powder microscopy images of the samples (inset) before and after the compression. (b) Absorption peak positions of the WO_3 nanoparticles under different pressures.

peaked at round 400 nm (cross marked in the figure), belonging to the coloration range of yellow-green, exhibited at atmospheric pressure. Increasing the pressure up to 4.0 GPa, we have found that the peak shifted gradually to a shorter wavelength (figure 3(a)). Above 4.0 GPa, the peak shifted to a longer wavelength. At the same time, the absorption peak at 4.0 GPa appears to be sharper than the other peaks between 0.5–7.9 GPa.

At the high-pressure range, the peak shifted to a shorter wavelength again at 9.8 GPa (figure 3(b)), however it constantly shifted to a longer wavelength except from the one at 25.0 GPa. Meanwhile, the peak shape varied with increased pressures. The downtrend of the absorption peak exhibited to a gentle slope at 31.8 GPa in contrast to the steep slope at 7.8 GPa, which might be caused by the appearance of new absorption peaks at higher wavelength.

Figure 4(a) shows the obvious spectra shape differences between the samples before and after the compression, and the post-compression sample exhibits an absorption of longer wavelength than the pristine sample. This result has shown that the pressure-induced coloration is irreversible, which has further confirmed by the actual color change from pale yellow (before compression, left) to dark blue (after compression, right) of the two samples (inset of figure 4(a)).

To further compare the spectra at different pressures, we plotted the absorption peak positions in figure 4(b). It is noted that the wavelength of the peaks are mostly increased with increased pressures, except from a few peaks from 0.5 to 2.4 GPa, 7.8–9.8 GPa, and 20.4–25.0 GPa.

4. Discussion

There is a correlation between the Raman spectra and UV–vis absorption spectra. In the Raman spectra, phase transitions around 9.4 GPa and 23.5 GPa have been observed, which corresponds to the decreased wavelengths

of the absorption peaks in figure 4, from 7.8 to 9.8 GPa and 20.4 to 25 GPa, respectively. Based on the Raman spectra, the first phase transition initiated at 0.3 GPa and finished at 1.6 GPa, which accounts for the wavelength decrease below 2.4 GPa in the absorption spectra. The phase transition results in the absorption peak shifting to lower wavelength, except from the one at 4 GPa which will be discussed later.

From figures 2 and 4(b), we note that the wavelength increases with increased pressure when no phase transition is involved. To account for this phenomenon, the relationship between the absorption spectra and band gap can be considered. High pressure leads to decreased atomic distances in the lattice that will affect the band gap. As a reflection of the bandgap of the WO_3, the position of absorption peak is therefore affected. Li *et al* have reported that the resistance decreased with increased pressure applied, except from at pressures where phase transition occurs [27, 28]. This means that the bandgap of WO_3 decreases with the increases of pressure under no phase change condition. Contributing to the absorption spectra, the decreases of the bandgap will cause the increase of the wavelength in the absorption peak.

We therefore consider the compression pressure having two combined ways affecting the absorption spectra of WO_3 nanoparticles. The anomalous absorption point at 4 GPa discussed earlier is a joint result of the two effects. At 4 GPa, the phase transition at around 3 GPa decreased the wavelength of absorption peak, but this effect is weaker than the increasing of wavelength caused by decreasing the bandgap under increased pressure. As a result, the wavelength still increases with pressure but grows less, which fits well with the experiment result.

By comparing figure 2(c) with figure 4, it is noted that the absorption spectra do not recover upon the release of pressure, due to the irreversible phase transition. We also notice that the spectrum after decompression look similar to that measured at 1.6 GPa. This may indicate that all high-pressure transitions are reversible and only this at 1.6 GPa seems irreversible, maybe due to pressure-induced defects and strains. The defects (oxygen vacancies) can also explain blue color after decompression. Meanwhile, the wavelength increase of the post-compression sample suggests a smaller bandgap in the WO_3 nanoparticles than the pristine sample. This analysis agrees with the result that WO_3 nanoparticles exhibit lower resistance after compression [28].

5. Conclusions

To summarize, we have found that the pressure-induced phase transition behavior of WO_3 nanoparticles is similar to those of microcrystalline WO_3, through the *in situ* high pressure Raman spectrum observations. The new phase change is irreversible during decompression. The irreversible pressure-induced chromism of WO_3 nanoparticles was also confirmed with UV–vis absorption spectra. The UV–vis measurement shows that the absorption peak wavelength increases with the pressure, which indicates a bandgap decrease due to shortening of the lattice parameters. The pressure-induced phase transition always accompanies with the absorption peak wavelength decreasing, and the pressure-induced chromism characteristic of the WO_3 nanoparticles is a combination of these two contributions. A pressure-structure-coloration relationship of WO_3 nanoparticles has therefore been established for up to 31.8 GPa.

Acknowledgments

We would like to acknowledge the support of NSAF (Grant No. U1530402). We also thank Prof Lin Wang of HPSTAR for the help in experiments.

ORCID iDs

Yanqiu Zhu https://orcid.org/0000-0003-3659-5643
Hao Yan https://orcid.org/0000-0002-3299-2417

References

[1] Shigesato Y 1991 Photochromic properties of amorphous WO_3 films *Japan. J. Appl. Phys.* **30** 1457–62
[2] Bechinger C *et al* 1994 The dynamics of the photochromic effect in tungsten trioxide *Solid State Commun.* **89** 205–7
[3] Xu N, Sun M, Cao Y W, Yao J N and Wang E G 2000 Influence of pH on structure and photochromic behavior of nanocrystalline WO_3 films *Appl. Surf. Sci.* **157** 81–4
[4] Avellaneda C O and Bulhões L O S 2003 Photochromic properties of WO_3, and WO_3 :X (X=Ti, Nb, Ta and Zr) thin films *Solid State Ion.* **165** 117–21
[5] Baeck S H *et al* 2003 Enhancement of photocatalytic and electrochromic properties of electrochemically fabricated mesoporous WO_3 thin films *Adv. Mater.* **15** 1269–73
[6] Deb S K 2008 Opportunities and challenges in science and technology of WO_3, for electrochromic and related applications *Solar Energy Materials & Solar Cells* **92** 245–58

[7] Avellaneda C O, Bueno P R and Bulhões L O S 2001 Synthesis and electrochromic behavior of lithium-doped WO_3, films *J. Non-Cryst. Solids* **290** 115–21
[8] Li F 2000 Preparation, characterization and photo-catalytic behavior of WO_3/TiO_2 nanopowder *Acta Phys.-Chim. Sin.* **16** 997–1002
[9] Deb S K 1973 Optical and photoelectric properties and colour centres in thin films of tungsten oxide *Phil. Mag.* **27** 801–22
[10] Miyazaki H, Ishigaki T and Ota T 2017 Photochromic smart windows employing WO_3-based composite films *Journal of Materials Science Research* **6** 62
[11] Wijs G A D and Groot R A D 1999 Structure and electronic properties of amorphous WO_3 *Phys.rev.* b **60** 16463–74
[12] Svensson J S E M and Granqvist C G 1985 Electrochromic coatings for smart windows: crystalline and amorphous WO_3 films *Thin Solid Films* **126** 31–6
[13] Boulova M and Lucazeau G 2002 Crystallite nanosize effect on the structural transitions of WO_3, studied by raman spectroscopy *J. Solid State Chem.* **167** 425–34
[14] Chen X *et al* 2011 Nanoarchitectonics of a Au nanoprism array on WO_3 film for synergistic optoelectronic response *Sci Technol Adv Mater* **12** 044604
[15] Liu X, Wang F and Wang Q 2012 Nanostructure-based WO_3 photoanodes for photoelectrochemical water splitting *Physical Chemistry Chemical Physics* **14** 7894–911
[16] Gullapalli S K, Vemuri R S and Ramana C V 2010 Structural transformation induced changes in the optical properties of nanocrystalline tungsten oxide thin films *Appl. Phys. Lett.* **96** 203508
[17] Locherer K R, Swainson I P and Salje E K H 1998 Transition to a new tetragonal phase of WO_3: crystal structure and distortion parameters *J. Phys. Condens. Matter* **11** 4143
[18] Howard C J, Luca V and Knight K S 2001 High-temperature phase transitions in tungsten trioxide–the last word? *J. Phys. Condens. Matter* **14** 377–87
[19] Salje E and Viswanathan K 1975 Physical properties and phase transitions in WO_3 *Acta Crystallographica* **31** 356–9
[20] Xu Y, Carlson S and Norrestam R 1997 Single crystal diffraction studies of WO_3 at high pressures and the structure of a high-pressure WO_3 phase *J. Solid State Chem.* **132** 123–30
[21] Salje E and Hoppmann G 1980 High-pressure transformations of tungsten trioxide *High Temperatures-High Pressures* **12** 213–6
[22] Filho A G S *et al* 2000 Pressure effects in the Raman spectrum of WO_3 microcrystals *Phys.rev.* b **62** 3699–703
[23] Boulova M *et al* 2002 High-pressure Raman study of microcrystalline WO_3 tungsten oxide *J. Phys. Condens. Matter* **14** 5849–63 (15)
[24] Bouvier P *et al* 2002 X-ray diffraction study of WO_3 at high pressure *J. Phys. Condens. Matter* **14** 6605–17
[25] Thummavichai K *et al* 2017 Low temperature annealing improves the electrochromic and degradation behavior of tungsten oxide (WO_x) thin films *J. Phys. Chem.* C **121** 20498–506
[26] Mao H K, Xu J and Bell P M 1986 Calibration of the ruby pressure gauge to 800 kbar under quasi-hydrostatic conditions *Journal of Geophysical Research Solid Earth* **91** 4673–6
[27] Li Y *et al* 2012 High-pressure electrical transport behavior in WO_3 *J. Phys. Chem.* C **116** 5210–5
[28] Li Y *et al* 2018 Investigation on electrical transport properties of nanocrystalline WO_3, under high pressure *J. Mater. Sci.* **53** 6339–49